Markov Chain Monte Carlo Defect Identification in NDE Images

Aleksandar Dogandži and Benhong Zhang

Citation: AIP Conference Proceedings **894**, 709 (2007); doi: 10.1063/1.2718040
View online: http://dx.doi.org/10.1063/1.2718040
View Table of Contents: http://scitation.aip.org/content/aip/proceeding/aipcp/894?ver=pdfcov
Published by the AIP Publishing

MARKOV CHAIN MONTE CARLO DEFECT IDENTIFICATION IN NDE IMAGES

Aleksandar Dogandžić and Benhong Zhang

Iowa State University, Center for Nondestructive Evaluation,
1915 Scholl Road, Ames, IA 50011, USA

ABSTRACT. We derive a hierarchical Bayesian method for identifying elliptically-shaped regions with elevated signal levels in NDE images. We adopt a simple elliptical parametric model for the shape of the defect region and assume that the defect signals within this region are random following a truncated Gaussian distribution. Our truncated-Gaussian model ensures that the signals within the defect region are higher than the baseline level corresponding to the noise-only case. We derive a closed-form expression for the kernel of the posterior probability distribution of the location, shape, and defect-signal distribution parameters (model parameters). This result is then used to develop Markov chain Monte Carlo (MCMC) algorithms for simulating from the posterior distributions of the model parameters and defect signals. Our MCMC algorithms are applied *sequentially* to identify multiple potential defect regions. For each potential defect, we construct Bayesian confidence regions for the estimated parameters. Estimated Bayes factors are utilized to rank potential defects (discovered by our sequential scheme) according to goodness of fit. The performance of the proposed methods is demonstrated on experimental ultrasonic C-scan data from an inspection of a cylindrical titanium billet.

Keywords: Bayesian analysis, defect identification, Markov chain Monte Carlo (MCMC).
PACS: 02.50.Tt Inference methods.

INTRODUCTION

In nondestructive evaluation (NDE) applications, defect signal typically affects multiple measurements at neighboring spatial locations and, consequently, multiple spatial measurements should be incorporated into defect identification algorithms [1], [2]. In [1], measurements within a sliding window are compared with a dynamically chosen threshold in order to detect potential defects in ultrasonic C scans. In [2], we propose a parametric model for defect shape, location, and signal parameters, a hierarchical Bayesian framework and Markov chain Monte Carlo (MCMC) algorithms for estimating these parameters assuming a singe defect, and a sequential method for identifying multiple defect regions. In this paper, we adopt a truncated-Gaussian defect-signal model that is more realistic than the Gaussian signal model in [2]: it ensures that the signals at *all* measurement locations within the defect region are above the baseline

CP894, *Review of Quantitative Nondestructive Evaluation Vol. 26,* ed. by D. O. Thompson and D. E. Chimenti

level corresponding to noise only. We then (i) derive a closed-form expression for the kernel of the posterior probability density function (pdf) of the *location, shape,* and *defect-signal distribution parameters* (termed *model parameters*), (ii) utilize this closed-form expression to develop efficient MCMC algorithms for simulating from the posterior distributions of the model parameters and defect signals, and (iii) apply our MCMC algorithms to identify multiple defect regions, estimate their parameters, and rank them according to goodness of fit. Remarkably, our MCMC algorithms developed herein are simpler to implement than those in [2], even though our measurement model (described in the following section) is more complex, as well as more realistic, than that in [2].

MEASUREMENT MODEL AND PRIOR SPECIFICATIONS

In this section, we introduce our defect location and shape models and random noise and defect-signal models. We then describe the prior model for the model parameters. Finally, we derive the kernel of the posterior pdf of the model parameters.

Parametric Model for Defect Location and Shape

We model a potential defect-signal region $\mathcal{R}(\boldsymbol{z})$ as an ellipse (see also [2]):

$$\mathcal{R}(\boldsymbol{z}) = \{\boldsymbol{r} : (\boldsymbol{r}-\boldsymbol{r}_0)^T \Sigma_{\mathrm{R}}^{-1} (\boldsymbol{r}-\boldsymbol{r}_0) \le 1\} \tag{1a}$$

where $\boldsymbol{r} = [x_1, x_2]^T$ denotes location in Cartesian coordinates, $\boldsymbol{z} = [\boldsymbol{r}_0^T, d, A, \varphi]^T$ is the vector of (unknown) defect location and shape parameters,

$$\Sigma_{\mathrm{R}} = \begin{bmatrix} \cos\varphi & -\sin\varphi \\ \sin\varphi & \cos\varphi \end{bmatrix} \begin{bmatrix} d^2 & 0 \\ 0 & A^2/(d^2\pi^2) \end{bmatrix} \begin{bmatrix} \cos\varphi & -\sin\varphi \\ \sin\varphi & \cos\varphi \end{bmatrix}^T \tag{1b}$$

and "T" denotes a transpose. Here, $\boldsymbol{r}_0 = [x_{0,1}, x_{0,2}]^T$ is the center of the ellipse in Cartesian coordinates, $d > 0$ is an axis parameter, A the area of the ellipse, and $\varphi \in [-\pi/4, \pi/4]$ the ellipse orientation parameter (in radians).

Measurement-Error (Noise) Model

Assume that we have collected measurements y_i at locations $\boldsymbol{s}_i$, $i = 1, 2, \ldots, \mathbb{N}_{\mathrm{tot}}$ within a region of interest, where $\mathbb{N}_{\mathrm{tot}}$ denotes the total number of measurement locations within this region. Denote by $\mathcal{N}(x\,;\,\mu,\sigma)$ the Gaussian pdf of a random variable x with mean μ and standard deviation σ. We adopt the simple additive white Gaussian noise model for the y_is (see also [2]):

$$p(y_i \,|\, \theta_i) = \mathcal{N}(y_i\,;\,\theta_i,\sigma), \quad i = 1, 2, \ldots, N \tag{2}$$

where θ_i are random *defect signals* when measurement locations $\boldsymbol{s}_i$ are within the potential defect-signal region [i.e. $\boldsymbol{s}_i \in \mathcal{R}(\boldsymbol{z})$] and $\theta_i = 0$ when $\boldsymbol{s}_i$ are in the noise-only part of the region of interest, denoted by $\mathcal{R}^{\mathrm{c}}(\boldsymbol{z})$. Here, we have set the baseline signal level (corresponding to the noise-only case) to zero, which can be done without loss of generality. If the baseline level is not zero (as, e.g., in C scans), we can subtract it out from the measurements, see also the numerical examples.

Defect-Signal (Reflectivity) Model

Denote by $\mathcal{N}_{\mathrm{t}}(x\,;\,\mu,\sigma)$ the truncated-Gaussian pdf of a random variable x with parameters μ and σ, where the truncation is made to restrict the range of x to non-

negative values:

$$\mathcal{N}_{\mathrm{t}}(x\,;\,\mu,\sigma) = \frac{\mathcal{N}(x\,;\,\mu,\sigma)}{\Phi(\mu/\sigma)} \cdot i_{[0,\infty)}(x) \tag{3a}$$

Here, $i_A(x) = \begin{cases} 1, & x \in A, \\ 0, & \text{otherwise} \end{cases}$ denotes the indicator function and $\Phi(\cdot)$ the cdf of the standard normal random variable. Assume that the defect signals $\{\theta_i,\, \boldsymbol{s}_i \in \mathcal{R}(\boldsymbol{z})\}$ are independent, identically distributed (i.i.d.) truncated Gaussian with unknown *defect-signal distribution parameters* μ and τ. Therefore, the joint pdf of the defect signals conditional on $\boldsymbol{z}$, μ, and τ is

$$p(\{\theta_i,\, \boldsymbol{s}_i \in \mathcal{R}(\boldsymbol{z})\} \,|\, \boldsymbol{z}, \mu, \tau) = \prod_{i,\ \boldsymbol{s}_i \in \mathcal{R}(\boldsymbol{z})} \mathcal{N}_{\mathrm{t}}(\theta_i\,;\,\mu,\tau). \tag{3b}$$

Note that τ is a measure of defect-signal variability; if $\tau = 0$, then all θ_i within the defect region are *equal to* μ, where $\mu > 0$. The above model imposes the non-negativity constraint on the signals from the defect region. In other words, the θ_is in the defect region are required to be higher than the zero baseline level. Define the vector of all model parameters $\boldsymbol{\phi} = [\boldsymbol{z}^T, \mu, \tau]^T$.

Prior Specifications for the Model Parameters $\boldsymbol{\phi}$

We assume that the defect location, shape, and signal-distribution parameters are independent *a priori*:

$$\pi_{\boldsymbol{\phi}}(\boldsymbol{\phi}) = \pi_{x_{0,1}}(x_{0,1}) \cdot \pi_{x_{0,2}}(x_{0,2}) \cdot \pi_d(d) \cdot \pi_A(A) \cdot \pi_\varphi(\varphi) \cdot \pi_\mu(\mu) \cdot \pi_\tau(\tau) \tag{4a}$$

and adopt simple uniform-distribution priors:

$$\pi_{x_{0,1}}(x_{0,1}) = \text{uniform}(x_{0,1,\text{MIN}}, x_{0,1,\text{MAX}}) \tag{4b}$$
$$\pi_{x_{0,2}}(x_{0,2}) = \text{uniform}(x_{0,2,\text{MIN}}, x_{0,2,\text{MAX}}) \tag{4c}$$
$$\pi_d(d) = \text{uniform}(d_{\text{MIN}}, d_{\text{MAX}}) \tag{4d}$$
$$\pi_A(A) = \text{uniform}(A_{\text{MIN}}, A_{\text{MAX}}), \quad \pi_\varphi(\varphi) = \text{uniform}(\varphi_{\text{MIN}}, \varphi_{\text{MAX}}) \tag{4e}$$
$$\pi_\mu(\mu) = \text{uniform}(0, \mu_{\text{MAX}}), \quad \pi_\tau(\tau) = \text{uniform}(0, \tau_{\text{MAX}}) \tag{4f}$$

where $\varphi_{\text{MIN}} \geq -\pi/4, \varphi_{\text{MAX}} \leq \pi/4, d_{\text{MIN}} > 0,\ A_{\text{MIN}} > 0$. Here, $\pi_{\boldsymbol{\phi}}(\boldsymbol{\phi})$ denotes the prior pdf of $\boldsymbol{\phi}$ and analogous notation is used for the prior pdfs of the components of $\boldsymbol{\phi}$.

Posterior Distribution of the Model Parameters $\boldsymbol{\phi}$

Define the vectors of random signals $\boldsymbol{\theta} = [\theta_1, \theta_2, \ldots, \theta_{\mathbb{N}_{\text{tot}}}]^T$ and measurements $\boldsymbol{y} = [y_1, y_2, \ldots, y_{\mathbb{N}_{\text{tot}}}]^T$ within the region of interest. We now derive a closed-form expression for the kernel of the posterior pdf of the model parameters $p(\boldsymbol{\phi} \,|\, \boldsymbol{y})$. Let us integrate out the signals $\boldsymbol{\theta}$ from the joint posterior pdf $p(\boldsymbol{\phi},\, \boldsymbol{\theta} \,|\, \boldsymbol{y})$:

$$p(\boldsymbol{\phi} \,|\, \boldsymbol{y}) = \frac{p(\boldsymbol{\phi},\, \boldsymbol{\theta} \,|\, \boldsymbol{y})}{p(\boldsymbol{\theta} \,|\, \boldsymbol{\phi},\, \boldsymbol{y})} \tag{5}$$

where $p(\boldsymbol{\phi},\, \boldsymbol{\theta} \,|\, \boldsymbol{y})$ and $p(\boldsymbol{\theta} \,|\, \boldsymbol{\phi},\, \boldsymbol{y})$ follow from the measurement model described above:

$$p(\boldsymbol{\phi},\, \boldsymbol{\theta} \,|\, \boldsymbol{y}) \propto \pi_{\boldsymbol{\phi}}(\boldsymbol{\phi}) \cdot p(\boldsymbol{\theta} \,|\, \boldsymbol{\phi}) \cdot p(\boldsymbol{y} \,|\, \boldsymbol{\theta}) \propto \pi_{\boldsymbol{\phi}}(\boldsymbol{\phi}) \cdot \Big[\prod_{i,\ \boldsymbol{s}_i \in \mathcal{R}(\boldsymbol{z})} \mathcal{N}_{\mathrm{t}}(\theta_i; \mu, \tau) \cdot \frac{\mathcal{N}(y_i; \theta_i, \sigma)}{\mathcal{N}(y_i; 0, \sigma)} \Big]$$

$$p(\boldsymbol{\theta} \,|\, \boldsymbol{\phi},\, \boldsymbol{y}) = \prod_{i,\ \boldsymbol{s}_i \in \mathcal{R}(\boldsymbol{z})} \mathcal{N}_{\mathrm{t}}\Big(\theta_i\,;\, \widetilde{\theta}_i(\mu,\tau), \Big(\frac{1}{\tau^2} + \frac{1}{\sigma^2}\Big)^{-1/2}\Big)$$

with
$$\widetilde{\theta}_i(\mu,\tau) = \frac{\tau^2\, y_i + \sigma^2\, \mu}{\tau^2 + \sigma^2}. \tag{6}$$

Substituting the above expressions for $p(\boldsymbol{\phi},\, \boldsymbol{\theta}\,|\,\boldsymbol{y})$ and $p(\boldsymbol{\theta}\,|\,\boldsymbol{\phi},\, \boldsymbol{y})$ into (5) yields

$$p(\boldsymbol{\phi}\,|\,\boldsymbol{y}) \propto \pi_{\boldsymbol{\phi}}(\boldsymbol{\phi}) \cdot l(\boldsymbol{y}\,|\,\boldsymbol{\phi}) \tag{7a}$$

where $l(\boldsymbol{y}\,|\,\boldsymbol{\phi})$ is the *likelihood function* of $\boldsymbol{\phi}$; the log-likelihood function of $\boldsymbol{\phi}$ [i.e. the logarithm of $l(\boldsymbol{y}\,|\,\boldsymbol{\phi})$] is

$$\begin{aligned} \ln l(\boldsymbol{y}\,|\,\boldsymbol{\phi}) \;\; &= \;\; -\frac{N(\boldsymbol{z})}{2}\, \ln\Big(1+\frac{\tau^2}{\sigma^2}\Big) \\ &\quad + \sum_{i,\; \boldsymbol{s}_i \in \mathcal{R}(\boldsymbol{z})} \Big\{ \ln\Big[\frac{\Phi\big(\widetilde{\theta}_i(\mu,\tau)\cdot\sqrt{\frac{1}{\tau^2}+\frac{1}{\sigma^2}}\big)}{\Phi(\mu/\tau)}\Big] + \frac{y_i^2}{2\,\sigma^2} - \frac{(y_i-\mu)^2}{2\,(\tau^2+\sigma^2)} \Big\} \end{aligned} \tag{7b}$$

where

$$N(\boldsymbol{z}) = \sum_{i,\, \boldsymbol{s}_i \in \mathcal{R}(\boldsymbol{z})} 1 \tag{7c}$$

denotes the number of measurements collected over $\mathcal{R}(\boldsymbol{z})$. Here, (7) follows by noting that $p(\boldsymbol{\phi}\,|\,\boldsymbol{y})$ *does not* depend on $\boldsymbol{\theta}$ and setting $\theta_i = \mu$ in the right-hand side of (5) [for i, $\boldsymbol{s}_i \in \mathcal{R}(\boldsymbol{z})$]. Setting the terms $\ln\big[\Phi\big(\widetilde{\theta}_i(\mu,\tau)\cdot\sqrt{\frac{1}{\tau^2}+\frac{1}{\sigma^2}}\big)/\Phi(\mu/\tau)\big]$ in (7b) to zero yields (logarithm of) the likelihood function in [2, eq. (3.1b)], which corresponds to the Gaussian defect-signal model; note that these terms are negative for negative y_i.

BAYESIAN ANALYSIS

We now develop MCMC methods for simulating from the posterior pdfs $p(\boldsymbol{\phi}\,|\,\boldsymbol{y})$ and $p(\boldsymbol{\theta}\,|\,\boldsymbol{y})$ of the model parameters and defect signals.

Simulating the Model Parameters $\boldsymbol{\phi}$

To draw samples from $p(\boldsymbol{\phi}\,|\,\boldsymbol{y})$, we apply a slice sampler [3] which creates an auxiliary random variable u and cycles between the following two steps:

Step 1: Draw a $u^{(t)}$ from uniform$\big(0, l(\boldsymbol{y}\,|\,\boldsymbol{\phi}^{(t-1)})\big)$ and

Step 2: Draw a $\boldsymbol{\phi}^{(t)}$ from its prior pdf $\pi_{\boldsymbol{\phi}}(\boldsymbol{\phi})$ *subject to* the indicator restriction

$$l(\boldsymbol{y}\,|\,\boldsymbol{\phi}^{(t)}) \geq u^{(t)}. \tag{8}$$

Let us now introduce some commonly used terminology. If a vector $\boldsymbol{\phi}$ satisfies the indicator restriction: $l(\boldsymbol{y}\,|\,\boldsymbol{\phi}) \geq u^{(t)}$, we say that it is *in the slice*. Consequently, Step 2 is referred to as "getting a point in the slice."

Step 2 Implementation. To get a point in the slice, we can apply a "naive" rejection method: keep drawing $\boldsymbol{\phi}$s i.i.d. from $\pi_{\boldsymbol{\phi}}(\boldsymbol{\phi})$ *until* we get a $\boldsymbol{\phi}$ that is in the slice. However, "naive" rejection may be very inefficient in terms of number of trials needed to get a point in the slice. Here, we utilize a more efficient *shrinkage sampling* approach [3]. First, recall that the parameter space of $\boldsymbol{\phi}$ is a *hyperrectangle* [see (4)], which defines the initial (largest) hyperrectangle in our shrinking scheme:

$x_{0,1,\mathrm{L}} = x_{0,1,\mathrm{MIN}}, x_{0,1,\mathrm{U}} = x_{0,1,\mathrm{MAX}}, x_{0,2,\mathrm{L}} = x_{0,2,\mathrm{MIN}}, x_{0,2,\mathrm{U}} = x_{0,2,\mathrm{MAX}}, d_{\mathrm{L}} = d_{\mathrm{MIN}}, d_{\mathrm{U}} = d_{\mathrm{MAX}}$
$A_{\mathrm{L}} = A_{\mathrm{MIN}}, A_{\mathrm{U}} = A_{\mathrm{MAX}}, \varphi_{\mathrm{L}} = \varphi_{\mathrm{MIN}}, \varphi_{\mathrm{U}} = \varphi_{\mathrm{MAX}}, \mu_{\mathrm{L}} = 0, \mu_{\mathrm{U}} = \mu_{\mathrm{MAX}}, \tau_{\mathrm{L}} = 0, \tau_{\mathrm{U}} = \tau_{\mathrm{MAX}}.$

We now obtain a $\boldsymbol{\phi}^{(t)}$ in Step 2 via the following sub-steps:

(a) Sample

$$\begin{array}{rlllrll} x_{0,1} & \text{from} & \text{uniform}(x_{0,1,\mathrm{L}}, x_{0,1,\mathrm{U}}), & & x_{0,2} & \text{from} & \text{uniform}(x_{0,2,\mathrm{L}}, x_{0,2,\mathrm{U}}) \\ d & \text{from} & \text{uniform}(d_{\mathrm{L}}, d_{\mathrm{U}}), & & A & \text{from} & \text{uniform}(A_{\mathrm{L}}, A_{\mathrm{U}}) \\ \varphi & \text{from} & \text{uniform}(\varphi_{\mathrm{L}}, \varphi_{\mathrm{U}}) & & \mu & \text{from} & \text{uniform}(\mu_{\mathrm{L}}, \mu_{\mathrm{U}}) \\ \tau & \text{from} & \text{uniform}(\tau_{\mathrm{L}}, \tau_{\mathrm{U}}) & & & & \end{array} \tag{9}$$

yielding $\boldsymbol{\phi} = [x_{0,1}, x_{0,2}, d, A, \varphi, \mu, \tau]^T$.

(b) Check if $\boldsymbol{\phi}$ is *within the slice*, i.e. if $l(\boldsymbol{y} \,|\, \boldsymbol{\phi}) \geq u^{(t)}$. (10)

If (10) holds, return $\boldsymbol{\phi}^{(t)} = \boldsymbol{\phi}$ and exit the loop.

(c) If (10) does not hold, then *shrink the hyperrectangle* so that $\boldsymbol{\phi}^{(t-1)}$ remains within it (since $\boldsymbol{\phi}^{(t-1)}$ is always in the slice):

- If $x_{0,1} < x_{0,1}^{(t-1)}$, set $x_{0,1,\mathrm{L}} = x_{0,1}$; else if $x_{0,1} > x_{0,1}^{(t-1)}$, set $x_{0,1,\mathrm{U}} = x_{0,1}$.
- If $x_{0,2} < x_{0,2}^{(t-1)}$, set $x_{0,2,\mathrm{L}} = x_{0,2}$; else if $x_{0,2} > x_{0,2}^{(t-1)}$, set $x_{0,2,\mathrm{U}} = x_{0,2}$.
- If $d < d^{(t-1)}$, set $d_{\mathrm{L}} = d$; else if $d > d^{(t-1)}$, set $d_{\mathrm{U}} = d$.
- If $A < A^{(t-1)}$, set $A_{\mathrm{L}} = A$; else if $A > A^{(t-1)}$, set $A_{\mathrm{U}} = A$.
- If $\varphi < \varphi^{(t-1)}$, set $\varphi_{\mathrm{L}} = \varphi$; else if $\varphi > \varphi^{(t-1)}$, set $\varphi_{\mathrm{U}} = \varphi$.
- If $\mu < \mu^{(t-1)}$, set $\mu_{\mathrm{L}} = \mu$; else if $\mu > \mu^{(t-1)}$, set $\mu_{\mathrm{U}} = \mu$.
- If $\tau < \tau^{(t-1)}$, set $\tau_{\mathrm{L}} = \tau$; else if $\tau > \tau^{(t-1)}$, set $\tau_{\mathrm{U}} = \tau$.
- Go back to (a).

Since evaluation of the likelihood $l(\boldsymbol{y} \,|\, \boldsymbol{\phi})$ may cause a floating-point underflow, it is safer to compute the log likelihood using (7b) and modify the shrinkage sampler accordingly, see [3, Sect. 4].

Simulating the Random Signals $\boldsymbol{\theta_i}$

To draw samples from $p(\boldsymbol{\theta} \,|\, \boldsymbol{y})$, we utilize *composition sampling* based on the identity $p(\boldsymbol{\theta} \,|\, \boldsymbol{y}) = \int p(\boldsymbol{\theta} \,|\, \boldsymbol{\phi}, \boldsymbol{y})\, p(\boldsymbol{\phi} \,|\, \boldsymbol{y})\, d\boldsymbol{\phi}$: draw $\boldsymbol{\phi}^{(t)}$ from $p(\boldsymbol{\phi} \,|\, \boldsymbol{y})$ as outlined in the previous section and then draw $\boldsymbol{\theta}^{(t)}$ from $p(\boldsymbol{\theta} \,|\, \boldsymbol{\phi}^{(t)}, \boldsymbol{y})$ as follows:

- for $i \in \mathcal{R}(\boldsymbol{z}^{(t)})$, draw conditionally independent samples $\theta_i^{(t)}$ from [see also (6)]

$$p(\theta_i^{(t)} \,|\, \boldsymbol{\phi}^{(t)}, y_i) = \mathcal{N}_{\mathrm{t}}\Big(\theta_i\,;\, \widetilde{\theta}_i(\mu^{(t)}, \tau^{(t)}), \Big[\frac{1}{(\tau^{(t)})^2} + \frac{1}{\sigma^2}\Big]^{-1/2}\Big),$$

- for $i \in \mathcal{R}^c(\boldsymbol{z}^{(t)})$, set $\theta_i^{(t)} = 0$,

yielding $\boldsymbol{\theta}^{(t)} = [\theta_1^{(t)}, \theta_2^{(t)}, \ldots, \theta_{\mathbb{N}_{\mathrm{tot}}}^{(t)}]^T$. Then, the mean signal $\overline{\theta} = [1/N(\boldsymbol{z})] \cdot \sum_{i,\, \boldsymbol{s}_i \in \mathcal{R}(\boldsymbol{z})} \theta_i$ within the potential defect region $\mathcal{R}(\boldsymbol{z})$ simulated in the tth draw is $\overline{\theta}^{(t)} = [1/N(\boldsymbol{z}^{(t)})] \cdot \sum_{i,\, \boldsymbol{s}_i \in \mathcal{R}(\boldsymbol{z}^{(t)})} \theta_i^{(t)}$. We also define the defect area to be proportional to the number of measurement locations $\boldsymbol{s}_i$ that are in the ellipse $\mathcal{R}(\boldsymbol{z})$ and have signals θ_i *within 10 dB* from the maximum signal θ_{MAX} in $\mathcal{R}(\boldsymbol{z})$, where $\theta_{\mathrm{MAX}} = \max_{i,\, \boldsymbol{s}_i \in \mathcal{R}(\boldsymbol{z})} \theta_i$. Consequently, defect area$^{(t)}$ corresponding to the tth draw is proportional to the number of $\theta_i^{(t)}$s in $\mathcal{R}(\boldsymbol{z}^{(t)})$ that are within 10 dB from $\theta_{\mathrm{MAX}}^{(t)} = \max_{i,\, \boldsymbol{s}_i \in \mathcal{R}(\boldsymbol{z}^{(t)})} \theta_i^{(t)}$.

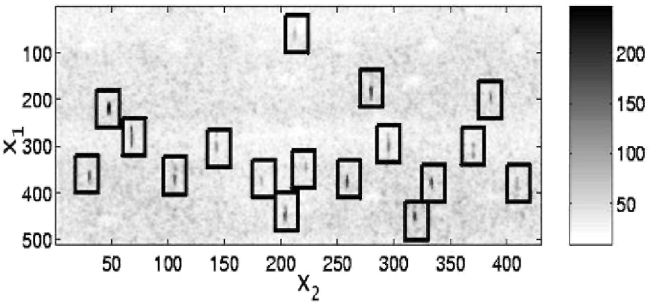

FIGURE 1. Ultrasonic C-scan data with 17 defects.

Estimating the Model Parameters ϕ and Random Signals θ

Once we have collected enough samples, we estimate the posterior means of $\boldsymbol{\phi}$ and $\boldsymbol{\theta}$ simply by averaging the last T draws:

$$\mathrm{E}\left[\boldsymbol{\phi} \,|\, \boldsymbol{y}\right] \approx \widehat{\boldsymbol{\phi}} = \frac{1}{T} \sum_{t=t_0+1}^{t_0+T} \boldsymbol{\phi}^{(t)}, \qquad \mathrm{E}\left[\boldsymbol{\theta} \,|\, \boldsymbol{y}\right] \approx \widehat{\boldsymbol{\theta}} = [\widehat{\theta}_1, \widehat{\theta}_2, \ldots, \widehat{\theta}_{\mathbb{N}_{\mathrm{tot}}}]^T = \frac{1}{T} \sum_{t=t_0+1}^{t_0+T} \boldsymbol{\theta}^{(t)} \quad (11)$$

where t_0 defines the burn-in period. Note that $\widehat{\boldsymbol{\phi}}$ and $\widehat{\boldsymbol{\theta}}$ are the (approximate) minimum mean-square error (MMSE) estimates of $\boldsymbol{\phi}$ and $\boldsymbol{\theta}$. Similarly, the MMSE estimates of $\overline{\theta}$ and defect area are obtained by averaging the quantities $\overline{\theta}^{(t)}$ and defect area$^{(t)}$.

Bayes Factor for Quantifying Goodness of Fit

We adopt the Bayes factor for comparing models $\mathrm{H}_0 : \mu = 0$ (defect absent) versus the alternative $\mathrm{H}_1 : \mu > 0$ (defect present) as a goodness-of-fit measure. This Bayes factor is simply the ratio of the marginal likelihoods under the hypotheses H_0 and H_1 (respectively) and can be estimated (up to a multiplicative constant) from the MCMC samples $\boldsymbol{\phi}^{(t)}$ using the approach in [4, Ch. 5.10.1]:

$$\mathrm{BF} \;\approx\; \frac{1}{T} \cdot \sum_{t=t_0+1}^{t_0+T} \frac{q(\boldsymbol{\phi}^{(t)})}{l(\boldsymbol{y} \,|\, \boldsymbol{\phi}^{(t)})\, \pi_{\boldsymbol{\phi}}(\boldsymbol{\phi}^{(t)})} \quad (12a)$$

where $q(\boldsymbol{\phi})$ is an arbitrary pdf having support within the support of the posterior pdf $p(\boldsymbol{\phi} \,|\, \boldsymbol{y})$. We select $q(\boldsymbol{\phi})$ to be a product of uniform pdfs:

$$q(\boldsymbol{\phi}) = q_{x_{0,1}}(x_{0,1}) \cdot q_{x_{0,2}}(x_{0,2}) \cdot q_d(d) \cdot q_A(A) \cdot q_\varphi(\varphi) \cdot q_\mu(\mu) \cdot q_\tau(\tau) \quad (12b)$$

obtained from the MCMC samples as follows: $q_{x_{0,1}}(x_{0,1}) = \mathrm{uniform}\big(\min\{x_{0,1}^{(t_0)}, x_{0,1}^{(t_0+1)}, \ldots, x_{0,1}^{(t_0+T)}\}, \max\{x_{0,1}^{(t_0)}, x_{0,1}^{(t_0+1)}, \ldots, x_{0,1}^{(t_0+T)}\}\big)$ and analogously for $q_{x_{0,2}}(x_{0,2})$, $q_d(d)$, $q_A(A)$, $q_\varphi(\varphi)$, $q_\mu(\mu)$, and $q_\tau(\tau)$. We use Bayes factors to compare multiple defect-region candidates: the candidates with smaller values of BF correspond to better fit.

NUMERICAL EXAMPLES

We apply the proposed approach to experimental ultrasonic C-scan data from an inspection of a cylindrical Ti 6-4 billet, see Fig. 1. Before analyzing the data, we divided the C-scan image into three regions of interest, as depicted in Fig. 2. In each

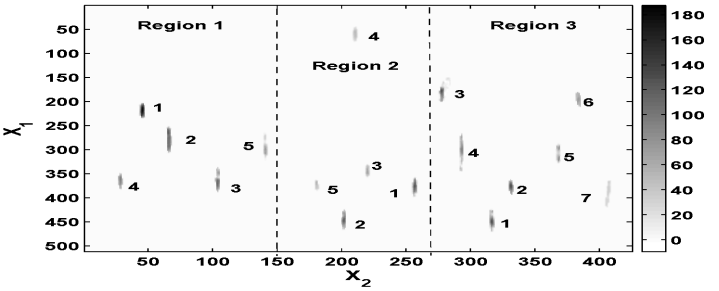

FIGURE 2. MMSE estimates $\widehat{\theta}_i$ of the random signals θ_i for the 17 chains having the smallest Bayes factors.

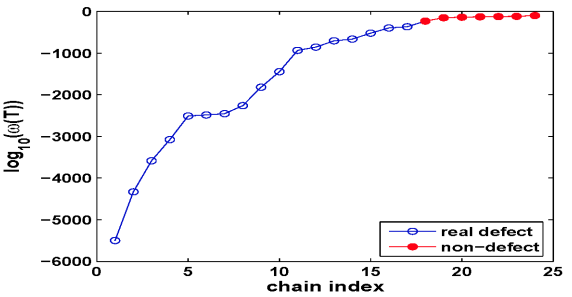

FIGURE 3. Logarithms of the estimated Bayes factors (up to an additive constant) for all 24 potential defects in the three regions of the inspected billet.

region, we subtracted row means from the measurements within the same row. The sample estimates of the noise variance σ^2 in Regions 1,2, and 3 are: $11.9^2, 10.3^2$, and 12.0^2, respectively. Further details about this data set and the outlined preprocessing steps are given in [2, Sect. IV]. We now analyze each region separately assuming known noise variances σ^2 (set to the above sample estimates). We chose the prior pdfs in (4d)–(4f) with $d_{\text{MIN}} = 1, d_{\text{MAX}} = 10, A_{\text{MIN}} = 20, A_{\text{MAX}} = 400$ (in squared pixels), $\varphi_{\text{MIN}} = -\pi/4, \varphi_{\text{MAX}} = \pi/4$ (covering the entire parameter space of φ, unlike [2]), $\mu_{\text{MAX}} = \max\{y_1, y_2, \ldots, y_{\mathbb{N}_{\text{tot}}}\}, \tau_{\text{MAX}} = 7\,\sigma$, and selected $x_{0,i,\text{MIN}}, x_{0,i,\text{MAX}}, i = 1, 2$ to span the region that is being analyzed.

We perform *sequential identification* of the potential defects as described in [2, Sect. IV], except that here we utilize the proposed slice sampler to draw $\boldsymbol{\phi}^{(t)}$ and $\boldsymbol{\theta}^{(t)}$. We have applied this sequential scheme to the three regions using 24 Markov chains (each running a slice sampler as described in this paper). For each chain, we ran $10,000$ cycles of the slice sampler and utilized the last $T = 2,000$ samples to describe the posterior distributions $p(\boldsymbol{\phi} \,|\, \boldsymbol{y})$ and $p(\boldsymbol{\theta} \,|\, \boldsymbol{y})$; hence, the burn-in period is $t_0 = 8,000$ samples. The estimated (and sorted) Bayes factors for all 24 chains, computed using (12), are shown in Fig. 3. Remarkably, the 17 smallest Bayes factors correspond to the chains that "discovered" the flat bottom holes (i.e. true defects) in Fig. 1. Fig. 2 shows the (overlaid) MMSE estimates $\widehat{\theta}_i$ of the defect signals estimated from these 17 chains.

In Fig. 4, we show approximate 90% Bayesian confidence regions for the normal-

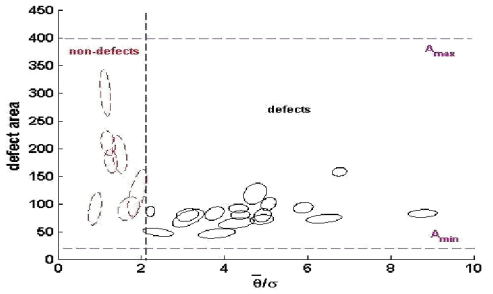

FIGURE 4. Approximate 90% Bayesian confidence regions for the normalized mean signals $\overline{\theta}/\sigma$ and areas of all potential defects in the three regions and a possible classification boundary for separating defects from non-defects.

ized mean signals $\overline{\theta}/\sigma$ and defect areas (in squared pixels)

$$\left([\text{defect area}, \frac{\overline{\theta}}{\sigma}] - [\widehat{\text{defect area}}, \frac{\widehat{\overline{\theta}}}{\sigma}]\right) C^{-1} \left([\text{defect area}, \frac{\overline{\theta}}{\sigma}]^T - [\widehat{\text{defect area}}, \frac{\widehat{\overline{\theta}}}{\sigma}]^T\right) \leq \xi \quad (13)$$

computed for all 24 potential defects in the three regions, where $\widehat{\text{defect area}}$ and $\widehat{\overline{\theta}}$ denote the MMSE estimates of the defect area and $\overline{\theta}$, C is the sample covariance matrix of the posterior samples $[\text{defect area}^{(t)}, \overline{\theta}^{(t)}/\sigma]^T$:

$$C = \frac{1}{T} \sum_{t=t_0+1}^{t_0+T} \left([\text{defect area}^{(t)}, \frac{\overline{\theta}^{(t)}}{\sigma}]^T - [\widehat{\text{defect area}}, \frac{\widehat{\overline{\theta}}}{\sigma}]^T\right)\left([\text{defect area}^{(t)}, \frac{\overline{\theta}^{(t)}}{\sigma}] - [\widehat{\text{defect area}}, \frac{\widehat{\overline{\theta}}}{\sigma}]\right)$$

and ξ is a constant chosen (for each chain) so that 90% of the samples $[\text{defect area}^{(t)}, \overline{\theta}^{(t)}/\sigma]^T$, $t = t_0, \ldots, T$ satisfy (13). In Fig. 4, we also show a *remarkably simple* classification boundary that successfully separates defects from non-defects, and is based only on the normalized mean signals $\overline{\theta}/\sigma$.

ACKNOWLEDGMENT

This work was supported by the NSF Industry-University Cooperative Research Program, Center for Nondestructive Evaluation (CNDE), Iowa State University.

REFERENCES

1. P.J. Howard, D.C. Copley, and R.S. Gilmore, "The application of a dynamic threshold to C-scan images with variable noise," in *Rev. Progress Quantitative Nondestructive Evaluation 17,* D.O. Thompson and D.E. Chimenti (Eds.), Plenum Press, NY, 1998, pp. 2013–2019.
2. A. Dogandžić and B. Zhang, "Bayesian NDE defect signal analysis," to appear in *IEEE Trans. Signal Processing*, **54**, (2006).
3. R.M. Neal, "Slice sampling," *Ann. Statist.,* **31**, 705–741 (2003).
4. M.-H. Chen, Q.-M. Shao, and J.G. Ibrahim, *Monte Carlo Methods in Bayesian Computation,* New York: Springer-Verlag, 2000.